

Circulation Research

JOURNAL OF THE AMERICAN HEART ASSOCIATION



Loss of Enigma Homolog Protein Results in Dilated Cardiomyopathy

Hongqiang Cheng, Kensuke Kimura, Angela K. Peter, Li Cui, Kunfu Ouyang, Tao Shen, Yujie Liu, Yusu Gu, Nancy D. Dalton, Sylvia M. Evans, Kirk U. Knowlton, Kirk L. Peterson and Ju Chen

Circ. Res. 2010;107;348-356; originally published online Jun 10, 2010;

DOI: 10.1161/CIRCRESAHA.110.218735

Circulation Research is published by the American Heart Association, 7272 Greenville Avenue, Dallas, TX 75214

Copyright © 2010 American Heart Association. All rights reserved. Print ISSN: 0009-7330. Online ISSN: 1524-4571

The online version of this article, along with updated information and services, is located on the World Wide Web at:

<http://circres.ahajournals.org/cgi/content/full/107/3/348>

Data Supplement (unedited) at:

<http://circres.ahajournals.org/cgi/content/full/CIRCRESAHA.110.218735/DC1>

Subscriptions: Information about subscribing to Circulation Research is online at
<http://circres.ahajournals.org/subscriptions/>

Permissions: Permissions & Rights Desk, Lippincott Williams & Wilkins, a division of Wolters Kluwer Health, 351 West Camden Street, Baltimore, MD 21202-2436. Phone: 410-528-4050. Fax: 410-528-8550. E-mail:
journalpermissions@lww.com

Reprints: Information about reprints can be found online at
<http://www.lww.com/reprints>

Loss of Enigma Homolog Protein Results in Dilated Cardiomyopathy

Hongqiang Cheng, Kensuke Kimura, Angela K. Peter, Li Cui, Kunfu Ouyang, Tao Shen, Yujie Liu, Yusu Gu, Nancy D. Dalton, Sylvia M. Evans, Kirk U. Knowlton, Kirk L. Peterson, Ju Chen

Rationale: The Z-line, alternatively termed the Z-band or Z-disc, is a highly ordered structure at the border between 2 sarcomeres. Enigma subfamily proteins (Enigma, Enigma homolog protein, and Cypher) of the PDZ-LIM domain protein family are Z-line proteins. Among the Enigma subfamily, Cypher has been demonstrated to play a pivotal role in the structure and function of striated muscle, whereas the role of Enigma homolog protein (ENH) in muscle remains largely unknown.

Objective:: We studied the role of Enigma homolog protein in the heart using global and cardiac-specific ENH knockout mouse models.

Methods and Results: We identified new exons and splice isoforms for ENH in the mouse heart. Impaired cardiac contraction and dilated cardiomyopathy were observed in ENH null mice. Mice with cardiac specific ENH deletion developed a similar dilated cardiomyopathy. Like Cypher, ENH interacted with Calsarcin-1, another Z-line protein. Moreover, biochemical studies showed that ENH, Cypher short isoform and Calsarcin-1 are within the same protein complex at the Z-line. Cypher short isoform and Calsarcin-1 proteins are specifically downregulated in ENH null hearts.

Conclusions: We have identified an ENH-CypherS-Calsarcin protein complex at the Z-line. Ablation of ENH leads to destabilization of this protein complex and dilated cardiomyopathy. (*Circ Res.* 2010;107:348-356.)

Key Words: Enigma homolog ■ ENH ■ dilated cardiomyopathy
■ Z-line ■ ENH-Cypher-Calsarcin-1 protein complex

The Z-line, also termed the Z-band or Z-disc, is an electron dense structure formed by multiple highly ordered protein complexes that is responsible for transmitting force between sarcomeres during contraction.^{1,2} The Z-line also connects myofibrils to the sarcolemmal membrane and ultimately the extracellular matrix.^{3,4} The Z-line is not only a basic structural anchor but also an important focus for signaling within striated muscle required for multiple aspects of muscle structure and function.^{5,6} Mutations in Z-line proteins have been linked to cardiomyopathy or myofibrillar myopathy both in humans and in transgenic mouse models.⁷⁻⁹

The Enigma subfamily members are Z-line proteins that interact directly with α -actinin-2. Enigma (PDLIM7 or LIM mineralization protein, LMP), Enigma homolog protein (also known as ENH or PDLIM5), and Cypher (ZASP in human) are 3 Enigma subfamily members that belong to the PDZ-LIM protein family.^{10,11} Cypher has been extensively studied by ourselves and others, and has been found to play a pivotal role in maintaining sarcomeric structure of striated muscle in humans and animals.^{8,12-19} Cypher-deficient mice die within 5 days after birth with multiple striated muscle defects, including dilated cardiomyopathy and disorganized Z-lines. Many mutations in

the human Cypher/ZASP gene have been identified in patients with dilated and/or hypertrophic cardiomyopathy.^{17,20-23} Recently, Cypher/ZASP mutations were also found in a portion of patients with myofibrillar myopathies, termed zaspopathy.^{8,24}

ENH, another member of the Enigma subfamily, is highly homologous to Cypher/ZASP and Enigma.²⁵⁻²⁷ In humans, there are 4 ENH splice isoforms that have been identified.²⁸ One long isoform (ENH1), containing 3 LIM domains at its C-terminus, has been found to be expressed ubiquitously in all tissues.^{26,27} Three short isoforms (ENH2-4) are expressed predominantly in cardiac and skeletal muscle.^{27,28} Splice isoforms of ENH are differentially expressed in heart during development and in heart diseases.²⁹ ENH has been reported to interact with α -actinin,^{25,28} protein kinase C,^{27,30,31} protein kinase D,³² L-type calcium channel,³² and a DNA transcription inhibitor, ID2.³³

We hypothesized that ENH, like its homologue Cypher, has an important role in the formation and/or maintenance of the normal Z-line in cardiac and skeletal muscle with an associated role in normal cardiac function. To begin to test this hypothesis, we analyzed ENH splice isoforms in the mouse heart and generated global and cardiac-specific ENH knockout mouse lines in which all ENH isoforms were

Original received February 10, 2010; revision received May 26, 2010; accepted June 1, 2010. In April 2010, the average time from submission to first decision for all original research papers submitted to *Circulation Research* was 15.2 days.

From the Department of Medicine, University of California—San Diego, La Jolla, Calif.

Correspondence to Ju Chen, PhD, Department of Medicine, University of California San Diego, 9500 Gilman Dr, La Jolla, CA 92093. E-mail juchen@ucsd.edu
© 2010 American Heart Association, Inc.

Circulation Research is available at <http://circres.ahajournals.org>

DOI: 10.1161/CIRCRESAHA.110.218735

ablated. We found wider Z-lines and dilated cardiomyopathy in ENH null mouse hearts. In addition, we identified that ENH forms a protein complex with Cypher short isoform (CypherS) and Calsarcin-1 at the Z-line. CypherS and Calsarcin-1 proteins are significantly downregulated in ENH-null mouse hearts resulting in wider and destabilized Z-lines, ultimately giving rise to dilated cardiomyopathy.

Methods

Targeted Disruption of Murine ENH

To generate a floxed allele targeting construct, a 682-bp PCR product containing exon 3 of ENH was cloned into a plasmid containing a Neomycin cassette and a diphtheria toxin A cassette. A 4.1-kb upstream fragment and a 4.4-kb downstream fragment were cloned into the vector as the 5'-arm or 3'-arm, respectively. The targeting vector was electroporated into R1 mouse ES cells derived from 129-SV/J mice (UCSD Transgenic and Gene Targeting Core, La Jolla, Calif). All subsequent procedures were performed in accordance with the NIH *Guide for the Care and Use of Laboratory Animals* and approved by the Institutional Animal Care and Use Committee of UCSD.

An expanded Methods section including all experimental procedures is available in the Online Data Supplement at <http://circres.ahajournals.org>.

Results

Multiple ENH Splice Isoforms in the Mouse Heart

To explore ENH function in the mouse and to ensure that all splice variants of ENH were accounted for in ENH-null mice, we first characterized the splice variants of ENH mRNA in

Non-standard Abbreviations and Acronyms	
cTnT-Cre	cardiac Troponin T Cre
cENH ^{-/-}	cardiac specific ENH knockout
CypherL	Cypher long isoforms
CypherS	Cypher short isoform
ENH	enigma homolog protein
FS	fractional shortening
LVID	left ventricular internal dimension
LVP	left ventricular pressure
LVPW	left ventricular posterior wall thickness
MHC	myosin heavy chain
NFAT	nuclear factor of activated T cells
WT	wild-type
ZASP	Z-band alternatively spliced PDZ motif protein

the mouse heart. Four mouse splice isoforms for ENH have been previously reported in the Ensembl database (Pdlim5-201 to Pdlim5-204) and 3 isoforms in NCBI data base (ENH1 to 3). After alignment we found the coding sequence of pdlim5-201 (1776 bp) is similar to ENH1 (NM_019808) (ENH1/1a in Figure 1), which is the ENH long isoform containing three C-terminal LIM domains. Pdlim5-202 (720 bp) is similar to ENH3 (ENH3b in Figure 1) (NM_022554) and pdlim5-203 (1014 bp) is similar to ENH2 (NM_019809). Pdlim5-204 (645 bp) is not listed in

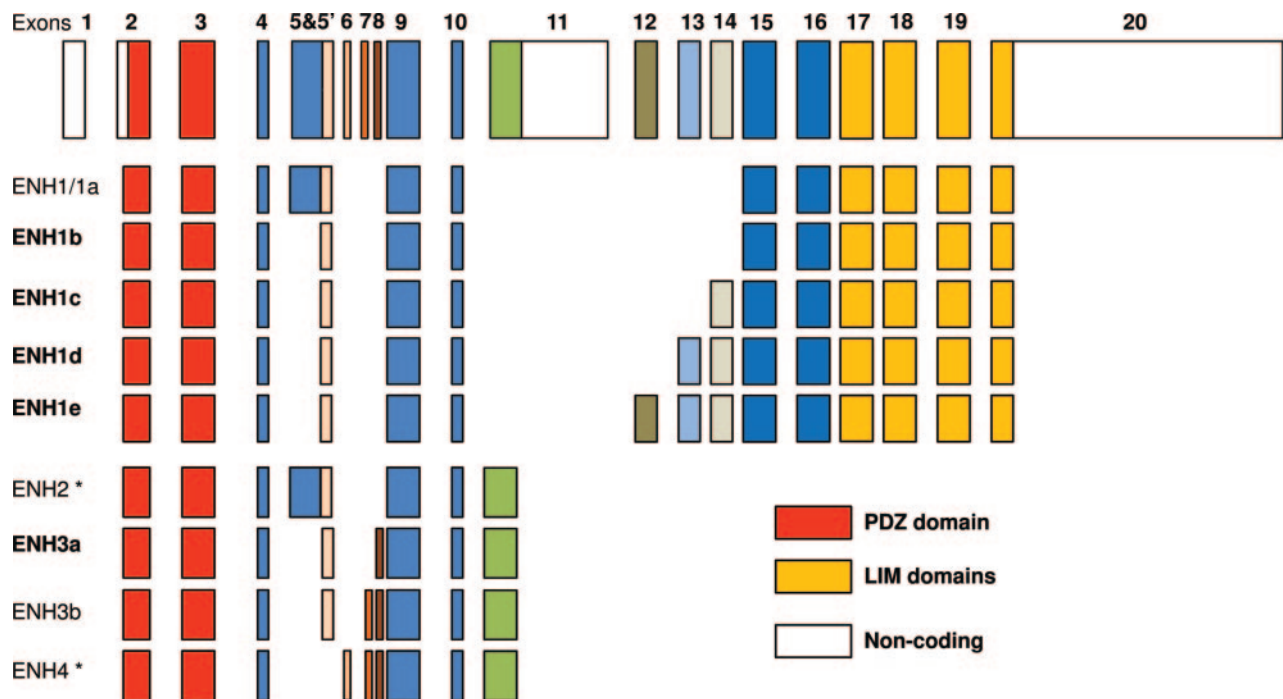


Figure 1. ENH genomic structure and splice isoforms. Colored boxes are used to represent the 20 exons that encode the murine ENH gene and blank boxes are noncoding regions. The translational start site is in the exon 2. Two stop codons for ENH gene are in exon 11 and exon 20, respectively. The N-terminal exons in red encode PDZ domain. The C-terminal exons in yellow encode 3 LIM domains. ENH1b is encoded using short exon 5' instead of exon 5 in ENH1/1a, which was reported as ENH1 in NCBI data base (NM_019808). Exons 12 to 14 are newly identified exons. ENH1c includes the short exon 5' and exon 14. ENH1d includes exon 5', exon 13, and exon 14. ENH1e includes exon 5' and exons 12 to 14. ENH4 includes the small 17-bp exon 6. ENH3b was renamed from ENH3 (NM_022554) and ENH3a does not include the small 15-bp exon 7. *ENH isoforms (ENH2 and ENH4) are only expressed in skeletal muscle.

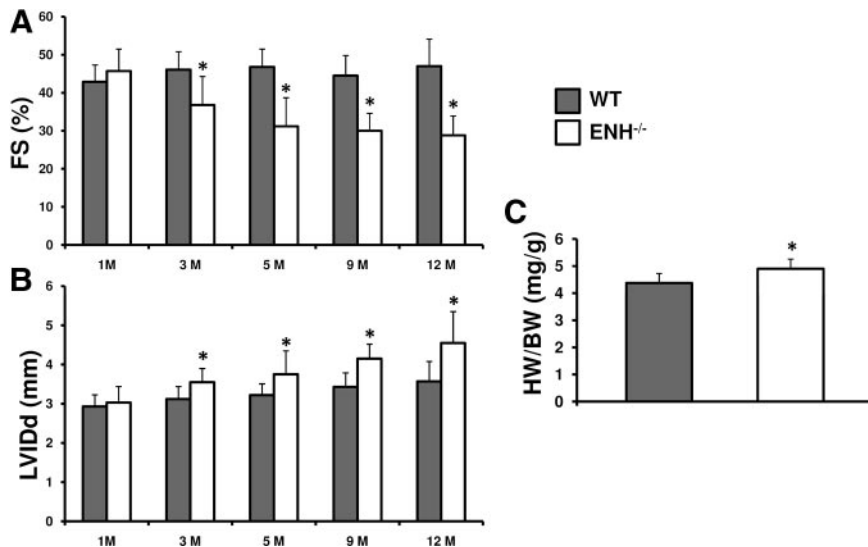


Figure 2. Dilated cardiomyopathy assessed by echocardiography in ENH^{-/-} mice. ENH^{-/-} mice (n=8, blank) and WT mice (n=8, gray) were measured at 1, 3, 5, 9, and 12 months of age. **A**, Reduced fractional shortening (FS) in ENH^{-/-} hearts (**P*<0.05). **B**, Enlarged left ventricles as shown by left ventricular internal dimension (LVIDd) at end diastole in ENH^{-/-} hearts (**P*<0.05). **C**, The ratios of heart weight-to-body weight (HW/BW) (mg/g) for ENH^{-/-} mice (male, n=5) and WT mice (male, n=5) at 3 months (**P*<0.05).

the NCBI database and is homologous to the newly identified human isoform ENH4.²⁸ ENH2, ENH3/3b and ENH4 are ENH short isoforms without the 3 LIM domains. Using primers for the full-length ENH short isoforms (ENH2–4), we failed to amplify ENH2 and ENH4 from mouse heart cDNA (Online Figure I A and I B). However, we identified ENH3b (we renamed ENH3 as ENH3b, Figure 1) and a new splice isoform with a deletion of exon 7, a small 15-bp exon in the mouse heart that we named ENH3a (Figure 1) (Online Figure I A). It should also be pointed out that we confirmed that ENH2 and ENH4 were expressed in skeletal muscle by RT-PCR and sequencing analysis (Online Figure I B).

To determine whether there are more ENH splice long isoforms, we performed RT-PCR analysis with primers in exon 9 and exon 16. By sequencing distinct PCR products, we discovered 3 previously unidentified exons, 12 to 14 (Figure 1 and Online Figure I C, D), containing 120 bp, 144 bp and 132 bp (Online Table I). RT-PCR analysis with primer pairs in exons 3 to 16 identified 4 novel ENH long isoforms (ENH1b, c, d, and e), and we renamed ENH1 as ENH1a (Figure 1 and Online Figure I D). As summarized in Figure 1, there are, in total, 9 splice isoforms for ENH in mouse striated muscle, among which there were 5 long isoforms with 3 LIM domains and 4 short isoforms without LIM domain. Short isoforms ENH2 and ENH4 are skeletal muscle-specific isoforms.

Generation of ENH-Null Mice

To investigate the *in vivo* biological role of ENH, we generated global ENH-null mice by ablating the third exon of the murine ENH gene. The detailed results and Figure are shown as Supplement Results and Online Figure II in the Online Data Supplement Material.

Dilated Cardiomyopathy in ENH-Null Mice

ENH^{-/-} mice are viable and are born at the expected mendelian ratios. ENH^{-/-} mice are fertile and are indistinguishable from wild-type (WT) littermates. We did not observe any mortality in ENH^{-/-} mice up to 2 years of age when the experiment was terminated. We first explored the heart performance by echocardiography for ENH^{-/-} mice

and WT control mice at various time points from 1 to 12 months (Figure 2). The left ventricular systolic function of ENH^{-/-} mice was impaired beginning at 3 months, as shown by a slight but significant enlargement of the left ventricle at end diastole (LVIDd) compared with WT mice beginning at 3 months (Figure 2B) and a decrease in fractional shortening (FS) (Figure 2A). However, there was no significant difference in wall thickness as indicated by both interventricular septum and left ventricular posterior wall thickness at end-diastole (data not shown). The heart weight-to-body weight ratio was mildly but significantly increased in ENH^{-/-} mice at 3 months (Figure 2C). In summary, the echocardiographic data shows ENH^{-/-} mice develop typical dilated cardiomyopathy beginning at 3 months with progressive deterioration but do not have sudden cardiac death.

We further assessed the dilated cardiomyopathy in ENH^{-/-} mice by measuring the mRNA levels of cardiac fetal genes (Figure 3A).³⁴ The expression of atrial natriuretic factor and skeletal α -actin were dramatically increased in the ENH^{-/-} hearts beginning at 1 month compared with age-matched WT mice. The fetal gene β -myosin heavy chain (MHC) was also increased significantly in ENH^{-/-} mouse hearts compared with controls. Thus, fetal gene expression was observed before the onset of dilated cardiomyopathy as measured by echocardiography.

Although chamber dilation and fetal gene expression patterns were significantly increased in ENH^{-/-} mouse hearts. We did not observe any myofibrillar disarray or fibrosis in 3-month-old ENH^{-/-} mice (Figure 3B and data not shown).

Because ENH has been shown to localize to the Z-line,²⁵ we performed transmission electron microscopy to examine Z-line organization (Figure 3C). In ENH^{-/-} mice, Z-lines were still intact but significantly wider compared with control mice (103.2±13.6 nm versus 77.4±6.1 nm; *P*≤0.003, respectively). The length of the sarcomeres and the width of the M-lines in ENH^{-/-} mice were comparable to that in control mice. These data showed deletion of ENH impaired the compact and ordered features of the Z-line structure.

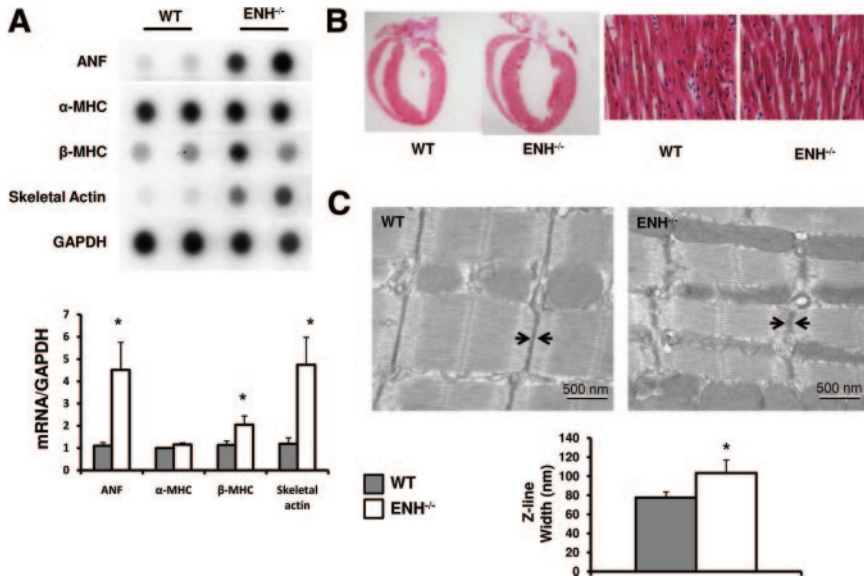


Figure 3. Characterization of the dilation and widened Z-lines in ENH^{-/-} mouse hearts. **A**, mRNA levels for cardiac fetal genes (atrial natriuretic factor, α-MHC, β-MHC and skeletal α-actin) was shown by dot-blot analysis of 1-month-old ENH^{-/-} male mice and WT controls. GAPDH was used as a RNA loading control. Quantification of RNA levels normalized to WT levels of the dot densities was shown in the **bottom panel** (**P*<0.05). **B**, Representative morphology of an ENH^{-/-} heart and WT heart at 3 months after hematoxylin and eosin stain. High-power field was shown in the **right panel** (×20). **C**, The ultra-structure of cardiac muscle from the left ventricles of 3-month-old WT and ENH^{-/-} mice was shown by electron microscopy. The quantitative width (distances between two **arrows**) of Z-lines is shown in the **bottom panel** (**P*<0.05).

Impaired Heart Contractility in ENH-Null Mice

Five-month-old male ENH^{-/-} and WT mice (n=8) underwent hemodynamic assessment. Contractile function of the heart was assessed by LV micromanometry (peak dP/dt) at rest and during stepped increases of dobutamine (β-adrenergic) stimulation. Both groups showed similar heart rates (Figure 4A) and peak left ventricular systolic pressure (LVP) (Figure 4B) under both basal conditions and after application of variable doses of dobutamine. The peak positive dP/dt (dP/dt max) was slightly but significantly decreased in ENH^{-/-} mice under high dobutamine concentrations (beginning at 4 μg · kg⁻¹ · min⁻¹) (Figure 4C). Isovolumic relaxation, as assessed by minimum dP/dt, was

dramatically impaired in ENH^{-/-} mice compared with WT controls at basal and various doses of dobutamine (Figure 4D). Also, the calculated Tau values in ENH^{-/-} mice were significantly longer than those in control mice (Figure 4E). These data suggested ENH^{-/-} mice failed to fully respond to dobutamine stimulation and exhibited myocardial inotropic and lusitropic dysfunction.

Dilated Cardiomyopathy in Cardiac-Specific ENH-Null Mice

To determine whether the dilated cardiomyopathy phenotype observed in the ENH global knockout mice was the result of

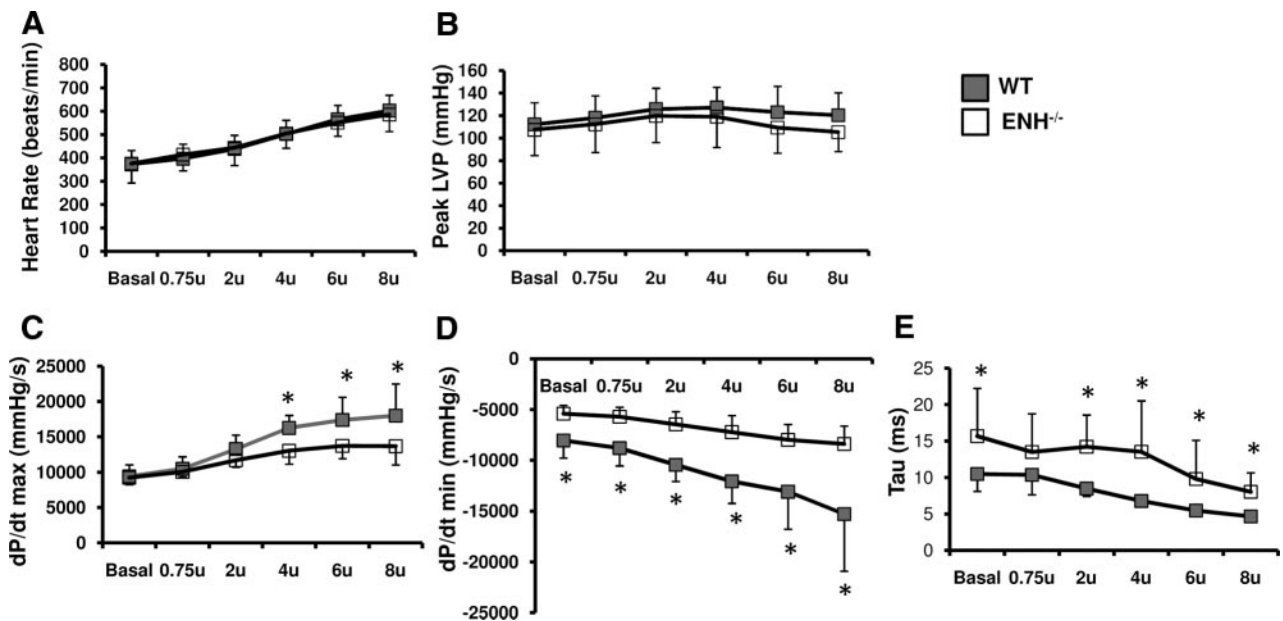


Figure 4. Impaired contractility in ENH^{-/-} hearts. Five-month-old male ENH^{-/-} (n=8) and WT mice (n=8) were subjected to hemodynamic measurements. **A and B**, ENH^{-/-} and WT mice had the same heart rates and maximum left ventricular pressure. **C**, ENH^{-/-} mice showed lower dP/dt maximum (dP/dt max) when stimulated with 4 to 8U (U=μg · kg⁻¹ · min⁻¹) of dobutamine (**P*<0.05). **D**, ENH^{-/-} mice had lower dP/dt minimum (dP/dt min) under basal conditions and with various doses of dobutamine (**P*<0.05). **E**, Tau, a load-independent measure of relaxation, was increased in ENH^{-/-} mice under basal conditions and after various doses of dobutamine ranging from 2 to 8 U (**P*<0.05).

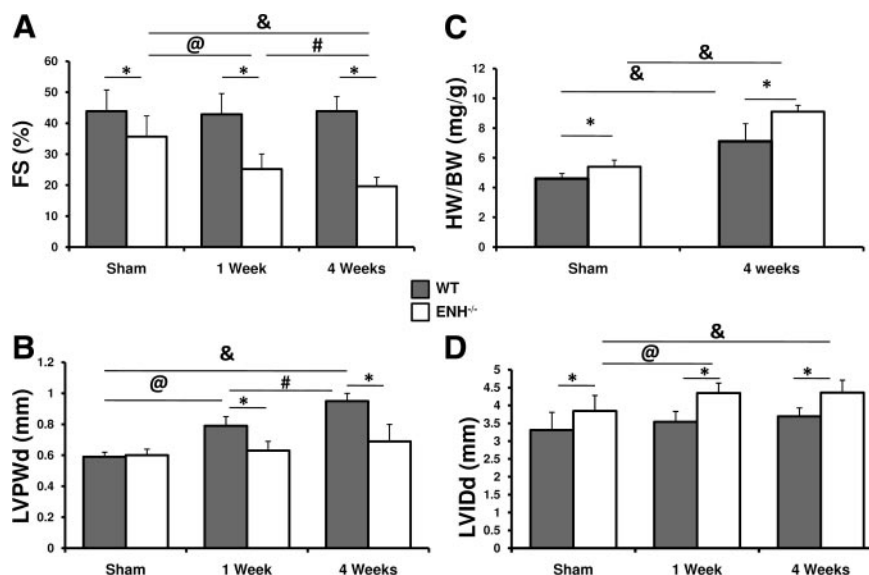


Figure 5. Increased systolic dysfunction in ENH-null mice after biomechanical stress. Two-month-old WT or ENH^{-/-} mice underwent either sham operation (n=3) or TAC surgery (n=8). **A**, Systolic heart function, as shown by percent fractional shortening (FS), was assessed by echocardiography. **B**, Left ventricular posterior wall thickness (LVPWd) at end of diastole is shown for sham, 1, and 4 weeks after TAC. **C**, Ratios of heart weight to body weight (HW/BW) are shown for sham and 4 weeks after TAC surgery. **D**, Left ventricular internal dimension (LVIDd) at end of diastole is shown for sham, 1, and 4 weeks after TAC. **P*<0.05 between WT and ENH^{-/-} groups. @*P*<0.05 between sham and 1 week after TAC. #*P*<0.05 between 1 week and 4 weeks after TAC. &*P*<0.05 between sham and 4 weeks after TAC.

the requirement for ENH in a cardiomyocyte autonomous fashion, we specifically deleted ENH in cardiomyocytes. The Troponin T-Cre mouse (cTnT-Cre), in which expression of *Cre* was controlled by the rat cardiac Troponin T promoter, was used to generate cardiac-specific ENH knockout mice.³⁵ To assess ENH protein expression in cardiac-specific knockout hearts, the ENH antibody from Abnova was used. Both ENH long and short isoforms were dramatically downregulated in the ENH cardiac-specific knockout hearts (Online Figure III A). As seen in the global ENH^{-/-} mice, the cardiac-specific ENH^{-/-} mice (cENH^{-/-}) developed dilated cardiomyopathy beginning at 3 months (Online Figure III B, C). The left ventricular function was significantly impaired in cENH^{-/-} hearts compared with control mice measured by FS (Online Figure III B). The left ventricular chamber size was enlarged significantly in cENH^{-/-} hearts (Online Figure III C), as indicated by LVID at both end diastole and end systole compared with cTnT-Cre carrier mice. There was no difference in ventricular wall thickness between cENH^{-/-} mice and cTnT-Cre mice (data now shown). Furthermore, as in global ENH^{-/-} hearts, the mRNA levels of cardiac fetal genes (atrial natriuretic factor, B-type natriuretic peptide, β -MHC, and skeletal α -actin) were dramatically increased in cENH^{-/-} hearts (Online Figure III D, E). The dilated cardiomyopathy in the cENH^{-/-} mouse suggested that the observed dilated cardiomyopathy and impaired left ventricular function in the global ENH^{-/-} mice were due to the loss of ENH in cardiomyocytes.

Increased Systolic Dysfunction in ENH-Null Mice After Biomechanical Stress

To assess cardiac function of ENH^{-/-} mice after biomechanical stress, we subjected mice to transverse aortic constriction (TAC). Significant decreases in left ventricular systolic function were observed beginning at 1 week after TAC in ENH^{-/-} mice when compared with WT mice and sham-operated ENH^{-/-} controls (Figure 5A). LVIDd was increased in TAC-banded ENH^{-/-} mice when compared with sham-operated or WT controls (Figure 5D). This was accompanied by a blunted increase in wall

thickness after pressure overload in ENH^{-/-} mice when compared with WT controls, as reflected by the LV posterior wall thickness (LVPWd) (Figure 5B) and interventricular septum thickness (data not shown). However, both ENH^{-/-} and WT mice displayed significant increases in HW/BW ratio (Figure 5C). Although ENH^{-/-} mice displayed a blunted LV posterior wall thickness, dilation was increased in TAC-banded ENH^{-/-} mice when compared with sham-operated or WT controls (Figure 5D).

Decreased Levels of Cypher Short Isoform and Calsarcin-1 in ENH-Null Heart

It has been shown that multiple intracellular signals are involved in sarcomeric protein deficiency-induced cardiomyopathy.³⁶ To determine molecular mechanisms underlying the dilated cardiomyopathy phenotype observed in ENH^{-/-} mice, we first checked stress related signaling pathways including, PKD, PKC, ERK, JNK, P38, AKT, and Calcineurin-NFAT in ENH-null mouse myocardium. No differences were observed in total or phosphorylated PKD, PKC, ERK, JNK, P38, and AKT between ENH^{-/-} and WT controls (Online Figure IV A, B). There was also no difference in calcineurin activity assayed by nuclear translocation of NFATc4 and the expression of its target gene, modulatory calcineurin-interacting protein, between ENH^{-/-} and WT controls (Online Figure V).

We then performed Western blot analysis for various Z-line proteins in ENH^{-/-} mice (Figure 6A). The CypherS and Calsarcin-1 were specifically downregulated in ENH^{-/-} mice at 3 months, and both proteins were nearly depleted at 12 months (Figure 6A and 6C). Interestingly, a small but significant decrease in CypherS and Calsarcin-1 was also detected in ENH mutants at 1 month, before the onset of dilated cardiomyopathy (Figure 6B and 6C). We have also found that with increased stress consequent to TAC, ENH mutants exhibit rapid loss of Calsarcin-1 and CypherS (Online Figure VI). This observation is correlated with more severe defects in cardiac contractile function in ENH mutants relative to control littermates (Figure 5).

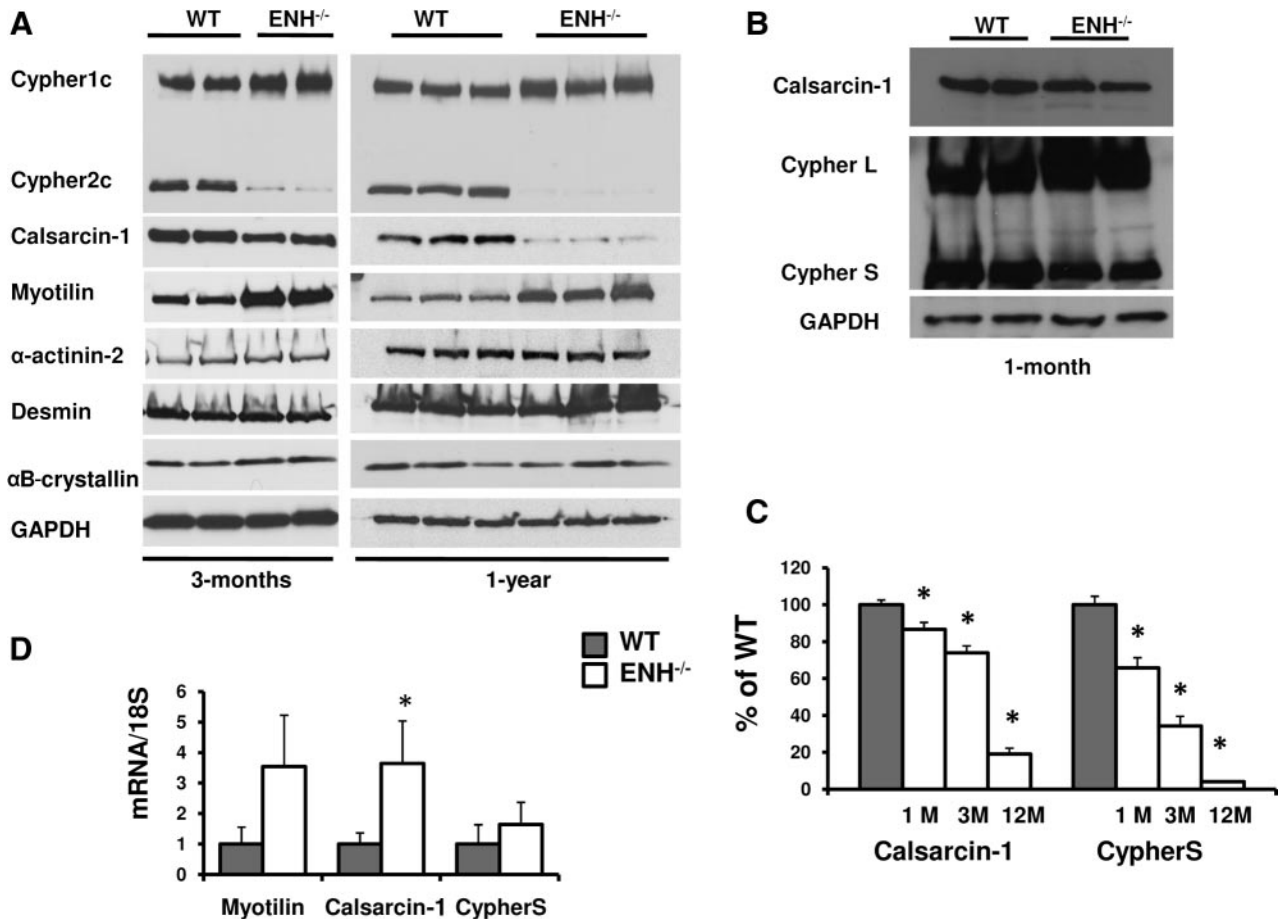


Figure 6. Loss of Cypher short isoform and Calsarcin-1 proteins in ENH^{-/-} hearts. **A**, CypherS and Calsarcin-1 were downregulated in 3-month-old ENH^{-/-} mice (**left panel**) and almost depleted in 12-month-old mice (**right panel**). Myotilin was unregulated in both 3-month-old and 12-month-old ENH^{-/-} mice. α B-crystallin, α -actinin 2, and Desmin were not different between WT and ENH^{-/-} mice at either age analyzed. GAPDH was shown as loading control. **B**, CypherS and Calsarcin-1 were slightly downregulated in 1-month ENH^{-/-} mice compared with age-matched WT controls. **C**, The downregulation of CypherS and Calsarcin-1 in ENH^{-/-} hearts is age dependent. **D**, The mRNA of Myotilin, Calsarcin-1 and CypherS were assessed by real-time RT-PCR. 18S RNA was used as internal RNA standard. The ratio to 18S RNA was further normalized to WT. * $P < 0.05$.

In ENH^{-/-} mice, Myotilin was upregulated. Amounts of other Z-line/Z-line associated proteins including α -actinin-2, Desmin, α B-crystallin and were not changed (Figure 6A). In contrast to the protein level, at the mRNA level, calsarcin-1 was significantly upregulated in ENH^{-/-} mice compared with controls (Figure 6D). Although not significant, mRNA expression of myotilin and cypherS was increased in ENH^{-/-} hearts (Figure 6D), suggesting that the loss of CypherS and Calsarcin-1 protein was due to a posttranslational mechanism and not due to decreased mRNA synthesis.

ENH-Cypher-Calsarcin-1 Protein Complex

To explore why CypherS and Calsarcin-1 proteins were specifically downregulated in ENH^{-/-} mice, we used a biochemical method to isolate myofibrillar proteins from 3-month-old adult mouse ventricles. As expected, cytosolic protein GAPDH and membrane protein Integrin β 1D were dominantly localized in the nonfilament fraction and sarcomeric protein Troponin I was dominantly localized in the filament fraction. These results for control proteins showed that this mild detergent washing method did specifically isolate the myofibril proteins from the heart (Figure 7A). We found the ENH short and long isoforms were

dominantly localized in the filament fraction as previously reported.²⁵ CypherL was found in both the filament and non-filament fractions, and CypherS was found dominantly in the filament fraction. The Z-line proteins Calsarcin-1 and Myotilin were also dominantly localized in the filament fraction in agreement with previously reported immunofluorescent data.^{37,38} In ENH^{-/-} hearts, Myotilin was highly increased in the filament fraction and could also be detected in the nonfilament fraction (Figure 7A).

To identify any possible protein complexes containing either Cypher or ENH, we performed a sedimentation assay. In sedimentation experiments, proteins that tightly interact with each other comigrate in the sucrose gradient and are localized in identical fractions. Our fractionation experiment showed that Calsarcin-1, CypherS, and ENH colocalize in fractions 1 to 3 in WT muscle (Figure 7B). When taken together with the loss of Calsarcin-1 and CypherS in the ENH^{-/-} mouse, the data indicate that these 3 proteins probably are localized within the same core complex. Interestingly, the fractionation patterns of both CypherL and Myotilin are similar, and both of these proteins are increased upon deletion of ENH. These data suggest that CypherL and

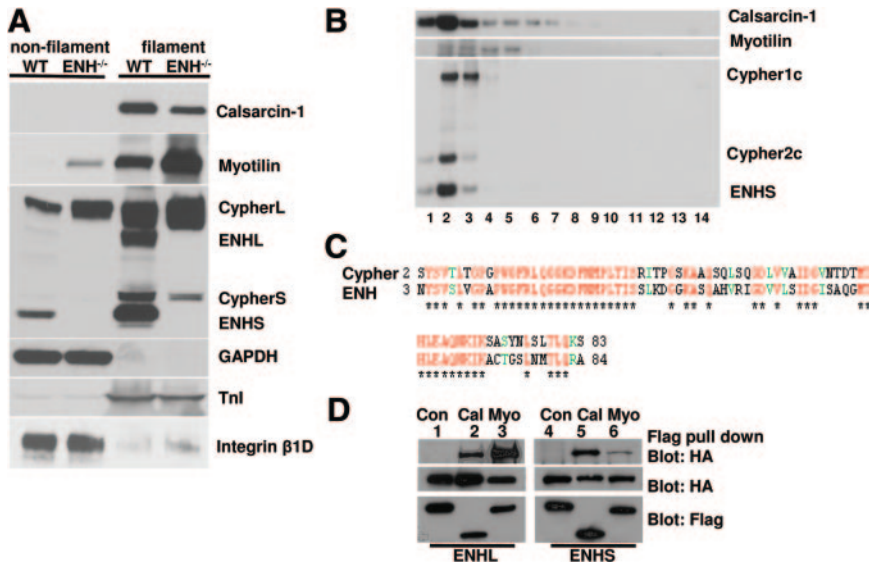


Figure 7. ENH-Cypher-Calsarcin protein complex. **A**, Calsarcin-1, Myotilin, CypherS, and ENH long isoforms were dominantly localized in the filament fraction as shown by biochemical isolation and Western blot analysis. CypherL and ENH short isoforms are in both filament and nonfilament fractions. GAPDH (cytosolic protein), Integrin β 1D (membrane protein) and Troponin I (Tnl, filament protein) were used as fractionation controls. **B**, ENH, CypherS, and Calsarcin are localized in the same fractions as shown by sucrose gradient sediment analysis. A total of 14 fractions were collected (from low to high of sucrose concentrations) and resolved by SDS-PAGE before Western blot analysis. **C**, The ENH PDZ domain shares high similarity in amino acid residues with the Cypher PDZ domain. Identical amino acid residues are shown in **red star** underneath and similar amino acid residues are shown in **green**.

for both the Cypher²⁻⁸³ and the ENH PDZ domains.³⁻⁸⁴ **D**, ENH interacted with Calsarcin-1 and Myotilin in vitro. FLAG-tagged Calsarcin-1 (lanes 2 and 5) or Myotilin (lanes 3 and 6) were coexpressed with HA-tagged ENH1 (ENH long isoform, lanes 1 to 3) or ENH3 (ENH short isoform, lanes 4 to 6) in HEK 293 cells. Exogenous protein expression was verified by immunoblotting with FLAG or HA antibodies. ANTI-FLAG M2 Affinity Gel was used to purify FLAG-tagged proteins and interacting proteins were visualized by immunoblotting with an HA antibody. FLAG-tagged control proteins (protein kinase A RI subunit) (lanes 1 and 4) were used as a control and did not bind to HA-tagged ENH proteins.

Myotilin may form a separate protein complex and may partially compensate for the loss of the ENH-CypherS-Calsarcin-1 protein complex in the ENH^{-/-} mouse.

We and others have reported that the Myotilin and Calsarcin-1 contain PDZ binding motifs at the C-terminus which interact with the PDZ domain of Cypher.^{16,39} Figure 7C shows 61% of identity (71% of similarity) between the Cypher PDZ domain and the ENH PDZ domain. We confirmed the interaction between ENH, Myotilin, and Calsarcin-1 in vitro (Figure 7D). Flag-tagged Calsarcin-1 interacted with both HA-tagged ENH1/1a and ENH3/3b, whereas a flag-tagged unrelated control protein, PKAR1 α , did not bind to either ENH isoform. Similar to Calsarcin-1, flag-tagged Myotilin interacted with both HA-tagged ENH1/1a and ENH3/3b. Along with the sedimentation assay results, these findings suggest that the filament proteins ENH, Cypher, and Calsarcin-1 form a protein complex through direct protein interactions.

Calsarcin has been shown to interact with Filamin C, which directly interacts with β 1 Integrin⁴⁰ and is associated with both γ and δ Sarcoglycan.⁴¹ Thus, the ENH-CypherS-Calsarcin complex at the Z-line may play a pivotal role in linking Z-lines to extracellular matrix via Filamin C. Loss of this complex may disrupt a critical structural function of the Z-line in establishing continuity between sarcomeres and the extracellular matrix to effect optimal force generation. To investigate this, we examined expression of Filamin C and components of structural complexes known to link sarcomeres to extracellular matrix, the Integrin and the Dystrophin glycoprotein complexes. Expression of Filamin C, β 1D Integrin, Dystrophin, Syntrophin, and γ Sarcoglycan were upregulated in ENH-null mice (Online Figure VII).

Discussion

Since the identification of the first PDZ-LIM domain protein (Enigma), a total of 10 PDZ-LIM domain protein members

have been identified in mammals.¹⁰ Based on sequence similarity and binding affinity, 4 subgroups have been identified within the PDZ-LIM protein family: Actinin-associated LIM protein, Enigma, LIM kinases, and LIM-domain only 7.¹⁰ Enigma, Cypher, and the closely related Enigma homolog (ENH) protein are members of the Enigma subfamily. Previously, using global and cardiac-specific knockout mouse models, we have demonstrated that Cypher is not necessary for sarcomerogenesis but is essential to maintain integrity of Z-line structure during muscular contraction.^{15,16} In the current report, we examined cardiac phenotypes of both global and cardiac-specific ENH knockout mice.

Before beginning our study, 4 ENH splice isoforms had been identified: ENH 1 to 4. In the current report, we have identified five additional previously undescribed ENH isoforms expressed in heart. All isoforms expressed in the mouse heart contain exon 3 which encodes part of the PDZ domain. For this reason, we chose to target exon 3 for deletion. Western blot results using different sources of antibodies demonstrated that ENH was absent in knockout mice. ENH knockout mice developed dilated cardiomyopathy characterized by enlargement of the left ventricle, impaired systolic and diastolic heart function, widened Z-lines, and elevation of fetal gene expression. Cardiac-specific knockout mice showed a similar dilated cardiomyopathy phenotype. In addition, we found that increased biomechanical stress consequent to TAC banding further exasperated the dilated cardiomyopathic phenotype. Together, these results suggest that ENH plays an important role in cardiac muscle structure and function.

Dilated cardiomyopathy is usually accompanied by activation of intracellular signaling pathways.⁴² In ENH^{-/-} mice, we failed to find activation of common cardiac stress pathways such as PKC, PKD, ERK, JNK, p38, AKT, and calcineurin-NFAT pathways at 3 months. By this age,

ENH^{-/-} mice showed enlarged hearts and widened Z-lines. Thus, the dilated phenotype observed with ENH mutants may reflect a structural requirement for ENH in the Z-line.

ENH, Cypher, and Calsarcin-1 directly interact with α -actinin-2 at the Z-line.^{12,25,37} Our results from myofibril isolation, sucrose fractionation, and in vitro pulldown assays demonstrate that ENH, CypherS, and Calsarcin-1 are components of a protein complex localized at the Z-line. In ENH knockout hearts, CypherS and Calsarcin-1 were specifically downregulated at the protein level but not at the mRNA level. Thus, deletion of ENH caused instability and loss of the CypherS/ENH/Calsarcin-1 protein complex. Calsarcin has been shown to interact with Filamin C, which directly interacts with β 1 Integrin⁴⁰ and is associated with both γ and δ Sarcoglycan.⁴¹ Thus, the ENH-CypherS-Calsarcin complex at the Z-line is likely to play a pivotal role in linking the Z-line to the extracellular matrix via Filamin C. Observed upregulation of Filamin C, Integrin, and components of the Dystrophin-glycoprotein complex in ENH mutants are likely to reflect a compensatory mechanism consequent to disruption of the connection between the Z-line and the extracellular matrix. Similar upregulation of these complexes has been shown to act as a compensatory mechanism to strengthen a weakened connection to the extracellular matrix in cardiac-specific β 1-Integrin knockout mice.⁴³

Taken together, our data suggest that loss of ENH leads to progressive loss of CypherS and Calsarcin resulting in the loss of Z-line structural integrity and consequent perturbation of the connection between adjacent sarcomeres and extracellular matrix. This leads to a loss of optimal force transmission and a significant decrease in fractional shortening and ultimately dilated cardiomyopathy.

Both Cypher and ENH knockout mice develop postnatal dilated cardiomyopathy, with differences in severity, hinting that there is a redundant but unique role for Cypher and ENH in the heart. Interestingly, in lower invertebrates, such as *Drosophila*, *Drosophila* ZASP (dZASP) is the only gene representing the entire actinin-associated LIM protein/Enigma subfamily of PDZ-LIM domain protein. dZASP is essential for *Drosophila* to form intact sarcomeres.^{18,19}

There appears to be substantial functional redundancy in proteins localized to the Z-line, as ablation of numerous Z-line proteins, including Calsarcin-1,⁴⁴ and Myotilin,⁴⁵ does not result in a significant basal phenotype. Both ENH and Cypher are expressed early in embryonic mouse heart (unpublished data).¹⁵ There is no obvious heart developmental defect in either ENH^{-/-} or Cypher^{-/-} mice, suggesting a possible functional overlap between these 2 Enigma family members during embryonic development. Future studies with ENH and Cypher double-mutant mice are needed to determine the potential role of ENH and Cypher in sarcomerogenesis and heart development.

Our findings that ENH plays an important role in the heart make it a novel disease candidate and suggest that human patients with cardiomyopathy should be screened for possible ENH mutations.

Sources of Funding

This work was supported by National Institutes of Health grants to J.C., K.L.P., S.M.E., and K.U.K., A.K.P. was supported by an American Heart Association Postdoctoral Fellowship award.

Disclosures

None.

References

1. Sanger JM, Sanger JW. The dynamic z bands of striated muscle cells. *Sci Signal*. 2008;1:pe37.
2. Goldstein MA, Schroeter JP, Michael LH. Role of the z band in the mechanical properties of the heart. *FASEB J*. 1991;5:2167–2174.
3. Towbin JA, Bowles NE. The failing heart. *Nature*. 2002;415:227–233.
4. Ervasti JM. Costameres: The Achilles' heel of Herculean muscle. *J Biol Chem*. 2003;278:13591–13594.
5. Kruger M, Linke WA. Titin-based mechanical signalling in normal and failing myocardium. *J Mol Cell Cardiol*. 2009;46:490–498.
6. Luther PK. The vertebrate muscle z-disc: sarcomere anchor for structure and signalling. *J Muscle Res Cell Motil*. 2009;30:171–185.
7. Frank D, Kuhn C, Katus HA, Frey N. Role of the sarcomeric z-disc in the pathogenesis of cardiomyopathy. *Future Cardiol*. 2007;3:611–622.
8. Selcen D, Carpen O. The z-disk diseases. *Adv Exp Med Biol*. 2008;642:116–130.
9. Clark KA, McElhinny AS, Beckerle MC, Gregorio CC. Striated muscle cytoarchitecture: an intricate web of form and function. *Annu Rev Cell Dev Biol*. 2002;18:637–706.
10. te Velthuis AJ, Bagowski CP. Pdz and lim domain-encoding genes: molecular interactions and their role in development. *Sci World J*. 2007;7:1470–1492.
11. Zheng M, Cheng H, Banerjee I, Chen J. Alp/enigma pdz-lim domain proteins in the heart. *J Mol Cell Biol*. 2010;2:96–102.
12. Zhou Q, Ruiz-Lozano P, Martone ME, Chen J. Cypher, a striated muscle-restricted pdz and lim domain-containing protein, binds to alpha-actinin-2 and protein kinase c. *J Biol Chem*. 1999;274:19807–19813.
13. Faulkner G, Pallavicini A, Formentin E, Comelli A, Ievolella C, Trevisan S, Bortoletto G, Scannapieco P, Salamon M, Mouly V, Valle G, Lanfranchi G. Zasp: a new z-band alternatively spliced pdz-motif protein. *J Cell Biol*. 1999;146:465–475.
14. Passier R, Richardson JA, Olson EN. Oracle, a novel pdz-lim domain protein expressed in heart and skeletal muscle. *Mech Dev*. 2000;92:277–284.
15. Zhou Q, Chu PH, Huang C, Cheng CF, Martone ME, Knoll G, Shelton GD, Evans S, Chen J. Ablation of cypher, a pdz-lim domain z-line protein, causes a severe form of congenital myopathy. *J Cell Biol*. 2001;155:605–612.
16. Zheng M, Cheng H, Li X, Zhang J, Cui L, Ouyang K, Han L, Zhao T, Gu Y, Dalton ND, Bang ML, Peterson KL, Chen J. Cardiac-specific ablation of cypher leads to a severe form of dilated cardiomyopathy with premature death. *Hum Mol Genet*. 2009;18:701–713.
17. Sheikh F, Bang ML, Lange S, Chen J. “Z” Eroding in on the role of cypher in striated muscle function, signaling, and human disease. *Trends Cardiovasc Med*. 2007;17:258–262.
18. Jani K, Schock F. Zasp is required for the assembly of functional integrin adhesion sites. *J Cell Biol*. 2007;179:1583–1597.
19. Benna C, Peron S, Rizzo G, Faulkner G, Megighian A, Perini G, Tognon G, Valle G, Reggiani C, Costa R, Zordan MA. Post-transcriptional silencing of the drosophila homolog of human zasp: a molecular and functional analysis. *Cell Tissue Res*. 2009;337:463–476.
20. Arimura T, Hayashi T, Terada H, Lee SY, Zhou Q, Takahashi M, Ueda K, Nouchi T, Hohda S, Shibutani M, Hirose M, Chen J, Park JE, Yasunami M, Hayashi H, Kimura A. A cypher/zasp mutation associated with dilated cardiomyopathy alters the binding affinity to protein kinase c. *J Biol Chem*. 2004;279:6746–6752.
21. Vatta M, Mohapatra B, Jimenez S, Sanchez X, Faulkner G, Perles Z, Sinagra G, Lin JH, Vu TM, Zhou Q, Bowles KR, Di Lenarda A, Schimmenti L, Fox M, Chrisco MA, Murphy RT, McKenna W, Elliott P, Bowles NE, Chen J, Valle G, Towbin JA. Mutations in cypher/zasp in patients with dilated cardiomyopathy and left ventricular non-compaction. *J Am Coll Cardiol*. 2003;42:2014–2027.
22. Moric-Janiszewska E, Markiewicz-Lozkot G. Genetic heterogeneity of left-ventricular noncompaction cardiomyopathy. *Clin Cardiol*. 2008;31:201–204.
23. Xing Y, Ichida F, Matsuoka T, Isobe T, Ikemoto Y, Higaki T, Tsuji T, Haneda N, Kuwabara A, Chen R, Futatani T, Tsubata S, Watanabe S, Watanabe K, Hirono K, Uese K, Miyawaki T, Bowles KR, Bowles NE, Towbin JA. Genetic analysis in patients with left ventricular noncompaction and evidence for genetic heterogeneity. *Mol Genet Metab*. 2006;88:71–77.

24. Griggs R, Vihola A, Hackman P, Talvinen K, Haravuori H, Faulkner G, Eymard B, Richard I, Selcen D, Engel A, Carpen O, Udd B. Zaspopathy in a large classic late-onset distal myopathy family. *Brain*. 2007;130:1477–1484.
25. Nakagawa N, Hoshijima M, Oyasu M, Saito N, Tanizawa K, Kuroda S. Enh, containing pdz and lim domains, heart/skeletal muscle-specific protein, associates with cytoskeletal proteins through the pdz domain. *Biochem Biophys Res Commun*. 2000;272:505–512.
26. Ueki N, Seki N, Yano K, Masuho Y, Saito T, Muramatsu M. Isolation, tissue expression, and chromosomal assignment of a human lim protein gene, showing homology to rat enigma homologue (enh). *J Hum Genet*. 1999;44:256–260.
27. Kuroda S, Tokunaga C, Kiyohara Y, Higuchi O, Konishi H, Mizuno K, Gill GN, Kikkawa U. Protein-protein interaction of zinc finger lim domains with protein kinase c. *J Biol Chem*. 1996;271:31029–31032.
28. Niederlander N, Fayein NA, Auffray C, Pomies P. Characterization of a new human isoform of the enigma homolog family specifically expressed in skeletal muscle. *Biochem Biophys Res Commun*. 2004;325:1304–1311.
29. Yamazaki T, Walchli S, Fujita T, Ryser S, Hoshijima M, Schlegel W, Kuroda S, Maturana AD. Splice variants of enigma homolog, differentially expressed during heart development, promote or prevent hypertrophy. *Cardiovasc Res*. 2010;86:374–382.
30. Maeno-Hikichi Y, Chang S, Matsumura K, Lai M, Lin H, Nakagawa N, Kuroda S, Zhang JF. A pkc epsilon-enh-channel complex specifically modulates n-type ca²⁺ channels. *Nat Neurosci*. 2003;6:468–475.
31. Chen Y, Lai M, Maeno-Hikichi Y, Zhang JF. Essential role of the lim domain in the formation of the pkepsilon-enh-n-type ca²⁺ channel complex. *Cell Signal*. 2006;18:215–224.
32. Maturana AD, Walchli S, Iwata M, Ryser S, Van Lint J, Hoshijima M, Schlegel W, Ikeda Y, Tanizawa K, Kuroda S. Enigma homolog 1 scaffolds protein kinase d1 to regulate the activity of the cardiac l-type voltage-gated calcium channel. *Cardiovasc Res*. 2008;78:458–465.
33. Lasorella A, Iavarone A. The protein enh is a cytoplasmic sequestration factor for id2 in normal and tumor cells from the nervous system. *Proc Natl Acad Sci U S A*. 2006;103:4976–4981.
34. Chien KR, Zhu H, Knowlton KU, Miller-Hance W, van-Bilsen M, O'Brien TX, Evans SM. Transcriptional regulation during cardiac growth and development. *Annu Rev Physiol*. 1993;55:77–95.
35. Jiao K, Kulesa H, Tompkins K, Zhou Y, Batts L, Baldwin HS, Hogan BL. An essential role of bmp4 in the atrioventricular septation of the mouse heart. *Genes Dev*. 2003;17:2362–2367.
36. Solaro RJ. Multiplex kinase signaling modifies cardiac function at the level of sarcomeric proteins. *J Biol Chem*. 2008;283:26829–26833.
37. Frey N, Richardson JA, Olson EN. Calsarcins, a novel family of sarcomeric calcineurin-binding proteins. *Proc Natl Acad Sci U S A*. 2000;97:14632–14637.
38. Salmikangas P, Mykkanen OM, Gronholm M, Heiska L, Kere J, Carpen O. Myotilin, a novel sarcomeric protein with two ig-like domains, is encoded by a candidate gene for limb-girdle muscular dystrophy. *Hum Mol Genet*. 1999;8:1329–1336.
39. von Nandelstadh P, Ismail M, Gardin C, Suila H, Zara I, Belgrano A, Valle G, Carpen O, Faulkner G. A class iii pdz binding motif in the myotilin and fatz families binds enigma family proteins: a common link for z-disc myopathies. *Mol Cell Biol*. 2009;29:822–834.
40. Gontier Y, Taivainen A, Fontao L, Sonnenberg A, van der Flier A, Carpen O, Faulkner G, Borradori L. The z-disc proteins myotilin and fatz-1 interact with each other and are connected to the sarcolemma via muscle-specific filamins. *J Cell Sci*. 2005;118:3739–3749.
41. Thompson TG, Chan YM, Hack AA, Brosius M, Rajala M, Lidov HG, McNally EM, Watkins S, Kunkel LM. Filamin 2 (fln2): a muscle-specific sarcoglycan interacting protein. *J Cell Biol*. 2000;148:115–126.
42. Liang Q, Molkentin JD. Redefining the roles of p38 and jnk signaling in cardiac hypertrophy: dichotomy between cultured myocytes and animal models. *J Mol Cell Cardiol*. 2003;35:1385–1394.
43. Elsharif L, Huang MS, Shai SY, Yang Y, Li RY, Chun J, Mekany MA, Chu AL, Kaufman SJ, Ross RS. Combined deficiency of dystrophin and beta1 integrin in the cardiac myocyte causes myocardial dysfunction, fibrosis and calcification. *Circ Res*. 2008;102:1109–1117.
44. Frey N, Barrientos T, Shelton JM, Frank D, Rutten H, Gehring D, Kuhn C, Lutz M, Rothermel B, Bassel-Duby R, Richardson JA, Katus HA, Hill JA, Olson EN. Mice lacking calsarcin-1 are sensitized to calcineurin signaling and show accelerated cardiomyopathy in response to pathological biomechanical stress. *Nat Med*. 2004;10:1336–1343.
45. Moza M, Mologni L, Trokovic R, Faulkner G, Partanen J, Carpen O. Targeted deletion of the muscular dystrophy gene myotilin does not perturb muscle structure or function in mice. *Mol cell biol*. 2007;27:244–252.

Novelty and Significance

What Is Known?

- The Enigma Homolog protein (ENH) is highly homologous to the proteins Cypher and Enigma.
- ENH has many splice isoforms. The long isoforms is expressed ubiquitously, whereas the short isoforms is expressed predominantly in cardiac and skeletal muscle.
- Mutations in Cypher lead to the development of dilated cardiomyopathy in both mice and humans.

What New Information Does This Article Contribute?

- It identifies previously unknown ENH exons and splice isoforms.
- It characterizes dilated cardiomyopathy and impaired cardiac function which develops in the absence of ENH.
- It identifies Z-line protein complex composed of ENH, Cypher short isoform, and Calsarcin-1.

The Enigma subfamily of proteins, including Cypher, Enigma, and ENH proteins, are localized to a highly ordered structure at

the border between neighboring sarcomeres, termed the Z-line. Cypher can play a pivotal role in maintaining striated muscle integrity in both humans and in mouse models. The role of ENH in striated muscle remains largely unknown. To investigate the role of ENH in mammalian cardiac muscle, we characterized and identified novel ENH splice isoforms in the mouse heart and generated global and cardiac-specific ENH knockout mouse lines in which all identified ENH isoforms were ablated. We found disorganized Z-lines and dilated cardiomyopathy in ENH knockout mouse hearts. Furthermore, we also found that ENH forms a protein complex with the Cypher short isoform and Calsarcin-1 at the Z-line and that the Cypher short isoform and Calsarcin-1 proteins are specifically downregulated in ENH knockout mouse hearts. We conclude that ablation of ENH leads to destabilization of this protein complex and consequent perturbation of the connection between adjacent sarcomeres and extracellular matrix, which leads to a loss of optimal force transmission and a significant decrease in fractional shortening and eventually dilated cardiomyopathy.

Supplement Material

Supplement Methods

Identification of Exons and Splice Isoforms of ENH

Ensembl and NCBI databases were used to search the reported ENH isoforms in the mouse genome. To confirm that the previously reported ENH short isoforms were present in the mouse heart, primers (ENH-SF: 5'-ATGAGCAACTACAGTGTGTC-3', and ENH-SR: 5'-TCACTGTACATTAAGAGCAC-3') were used to amplify ENH short isoforms (ENH3, NM_022554) from adult mouse heart cDNA. Each resultant PCR product was cloned into the pCR[®]-Blunt II-TOPO[®] cloning vector (Invitrogen, Carlsbad, CA) and sequenced. For ENH long isoforms, we first designed primers in exon 9 (ENHE9: 5'-TCACTGGGACTGAGCATCTG-3') and exon 16 (ENHE16: 5'-TCCCCTGATAACTTGGTTGC-3'). All PCR products were cloned and sequenced as stated above. To determine whether ENH had a previously unidentified, extra transcriptional start site, the primer pair ENH-SF and ENHE16 were used. Again, all PCR products were cloned and sequenced as described above.

Targeted Disruption of Murine ENH

The targeting vector was constructed using a plasmid containing a Neomycin cassette flanked by two *Frt* sites.¹ To generate a floxed allele targeting construct, a 682 bp PCR product containing exon 3 of ENH was cloned into the *Bam*H I site flanked by two *loxP* sites. A 4.1-kb upstream fragment and a 4.4-kb downstream fragment were cloned into the vector as the 5'-arm or 3'-arm, respectively. The targeting vector was linearized with *Not* I and electroporated into R1 mouse ES cells derived from 129-SV/J mice (UCSD Transgenic and Gene Targeting Core, La Jolla, CA). After G418 selection, homologous recombinants were identified by digesting genomic DNA with *Bam*H I followed by Southern blot analysis. The WT allele was represented as a 25-kb band, whereas the 15-kb band represented a targeted allele. All PCR was performed utilizing the high-fidelity KOD Hot Start DNA polymerase (Novagen, Gibbstown, NJ). All PCR products were cloned into a pCR[®]-Blunt II-TOPO[®] vector (Invitrogen, Carlsbad, CA), and the sequence was verified. The 3'-probe (453 bp) used for Southern blot analysis was generated by PCR using ProbeF (5'-AAAACAAAACAGTGAACAGAGCAG-3') and ProbeR (5'-TGGTCCATCCTTATTTACTAGGC-3') as primers. A diphtheria toxin A (DTA) expression cassette was placed at the 3' end of the targeting construct to facilitate the rate of homologous recombination.

Two positive ES cell clones with a floxed ENH exon 3 were microinjected into C57BL/6 blastocysts and transferred to pseudo-pregnant recipients. Male chimeras were mated with Black Swiss females (Taconic Inc, Hudson, NY), and agouti offspring were genotyped by PCR and Southern blot analysis of tail DNA. After germline transmission of the targeted allele was confirmed, heterozygous mice (ENH^{f/+}) were obtained by crossing targeted mice (ENH^{f/+}) with protamine-Cre mice.² Homozygous knockout (ENH^{-/-}) mice were generated by intercrossing two heterozygous mice. Genotypes were determined by PCR using primers P1 (5'-GCAGGAAGCACACCCAGTAT-3') versus P2 (5'-TGGTCTCCAACATTTACCA-3') for WT and Frtneo (5'-AATGGGCTGACCGCTTCCTCGT-3') versus P4 (5'-TCGGATGGATGCTCTTCT-3') for knockout. The WT allele band was 308 bp, the floxed allele gave a product of 378 bp, and the knockout allele was 561 bp.

To generate cardiac-specific ENH^{-/-} mice (cENH^{-/-}), cardiac troponin T Cre³ heterozygous mice were crossed with ENH^{f/+} mice to get ENH^{f/+}, Cre mice. ENH^{f/+}, Cre male mice were subsequently

bred with ENH^{ff} female mice to get ENH^{ff, Cre} mice, which were the cardiac specific ENH^{-/-} mice (cENH^{-/-}) and ENH^{ff+, Cre} mice, which here were used as controls.

All procedures were performed in accordance with the NIH *Guide for the Care and Use of Laboratory Animals* and approved by the Institutional Animal Care and Use Committee of UCSD.

Echocardiography and Hemodynamic Measurements

Echocardiography was performed while under anesthesia with isoflurane (5% in pure oxygen for 1 min and then maintained at 1% isoflurane) using a Philips, Sonos 5500 machine (Philips Medical Systems, Andover, MA) with a 15-MHz transducer. Data for LV chamber dimensions (LVID), left ventricular posterior wall thickness (LVPW), and interventricular septum thickness (IVS), were recorded at end diastole and end systole. Heart contractility, shown as percentage of fractional shortening of the LV (%FS), was calculated as described previously⁴.

Hemodynamic evaluation was performed while animals were under general anesthesia (100 mg/kg ketamine and 5 mg/kg xylazine) while connected to a ventilator. 3-month-old male mice (n=8 in each group) were subjected to i.v. stimulation with various doses of dobutamine (U=μg/kg/min), a β-adrenergic agonist, and cardiac performance was detected as described previously.⁵ The following parameters were averaged from 12 beats: heart rate; maximum end-systolic LV pressure (LVP); maximum positive and negative first derivative of LVP (dP/dt); and exponential Tau, using a linear regression fit of the relation between dP/dt and pressure during isovolumic pressure decline.

Transverse Aortic Constriction (TAC)

2-month-old mice either under sham operation or induced pressure overload by transverse aortic constriction (TAC) as described previously.⁶ Heart function was measured by echocardiography at 1 and 4 weeks after surgery and pressure gradient produced by TAC was measured at the end of experiment.

RNA Isolation, Dot-blot Assay and Real-time RT-PCR

Total RNA was isolated from mouse ventricles using TRIzol[®] reagent (Invitrogen, Carlsbad, CA) following the manufacture's protocol. RNA dot-blot was performed as previously described⁷. Quantitation of RNA levels was performed using ImageJ software. cDNA was synthesized using ThermoScript[™] RT-PCR System (Invitrogen, Carlsbad, CA) with the oligo dT primer. Real-time PCR was performed using the IQ5 Real-time PCR Detection System (BioRad, Hercules, CA) using SYBR[®] Green PCR Master Mix (Applied Biosystems, Foster City, CA).

Transmission Electron Microscopy

Transmission electron microscopy (TEM) was performed as described previously⁸ at the National Center for Microscopy and Imaging Research, UCSD. Briefly, mice were injected with heparin (0.5 ml, 100 U/ml) and anesthetized with Nembutal (40 μl, 50 mg/μl). The chest was then opened to expose the heart, and an incision was made in the right atrium. The mice were perfused through the left ventricle with 50 mM KCl in phosphate buffered saline followed by fixation (2% paraformaldehyde, 2% glutaraldehyde in 0.15 M sodium cacodylate buffer, pH 7.4). Subsequently, the heart was removed, cut into smaller pieces, and kept in fixative for 4 hrs. Tissue was post-fixed in 1% OsO₄ in 0.15 M sodium cacodylate buffer for 90 min, at 4 °C, and dehydrated in a graded series of ethanol and acetate. Tissue was embedded into Durcupan resin (EMD, Gibbstown, NJ). Ultrathin sections were stained with uranyl acetate and lead citrate. Electron micrographs were recorded using a JEOL 1200EX electron microscope (JEOL Ltd).

Tokyo, Japan) operated at an accelerating voltage of 80 kV. To measure the width of the Z-line, we used software developed in our laboratory to calculate the distance between two points (depicted by arrows in the manuscript figure). The width of each Z-line was averaged from 3 different points (one on either end of the Z-line and one centralized point). Three ENH^{-/-} mice and two WT mice were analyzed. In total, over 100 Z-lines were measured for both groups.

Histology and Staining

Hearts were freshly harvested, relaxed in 50 mM KCl in phosphate buffered saline, and then fixed in 4% paraformaldehyde in phosphate buffered saline. Hearts were embedded in paraffin after dehydration by ethanol and cleared in xylene. Hematoxylin and eosin (H&E) staining was performed according to standard procedures.⁹ Trichrome stain was performed as recommended by the manufacturer (Sigma-Aldrich, St. Louis, MO).

Myofibril Protein Isolation, Cellular Fraction, Protein Extraction, and Western Blots

Myofibril proteins were isolated from 3-month-old mouse ventricles as previously described.¹⁰ In short, freshly harvested mouse ventricles were cut into small pieces before homogenization with a dounce homogenizer in 4 volumes of buffer A (0.3 M sucrose and 10 mM imidazole, pH 7.0). The homogenate was centrifuged at 17,300 x g, for 20 min, at 4 °C. This first supernatant was labeled as non-filament proteins. Pellet was resuspended in the same initial volume of buffer B (60 mM KCl, 30 mM imidazole, 2 mM MgCl₂, 2 mM EGTA, 1% Triton X-100, pH 7.0) with the addition of a protease inhibitor tablet (Roche, Basel, Switzerland). The suspension was homogenized again and centrifuged at 750 x g, for 15 min. In total, this wash procedure was repeated at minimum six times. The resultant pellet was labeled as filament proteins. Protein concentration was determined by the DC protein assay kit (BioRad, Hercules, CA) and samples were resolved by SDS-PAGE. Proteins were transferred to PVDF membrane for further immunoblotting.

For sucrose gradient fractionation, 5-week-old WT cardiac tissue was snap frozen in liquid nitrogen and ground to a fine powder with a mortar and pestle. Pulverized cardiac tissue was then added to ice-cold modified RIPA lysis buffer with phosphatase inhibitors (1% Nonidet P-40, 0.5% sodium deoxycholate, 0.1% SDS, 1 mM EDTA, 5 mM N-ethylmaleimide, 50 mM sodium fluoride, 2 mM b-glycerophosphate, 1 mM sodium orthovanadate, 100 nM okadaic acid, 5 nM microcystin LR, and 20 mM Tris-HCL, pH 7.6) and protease inhibitors (0.6 ug/mL pepstatin A, 0.5 ug/mL aprotinin, 0.5 ug/mL leupeptin, 0.75 mM benzamidine, and 0.1 mM PMSF). Tissue homogenate was then subjected to mechanical homogenization using a Polytron PT 2000 bench top homogenizer (Kinematica, Lucerne, Switzerland). Homogenate was rocked at 4°C for 1 hr. Following clarification by centrifugation at 15,000 x g for 15 min, the concentration of the tissue lysate was measured as stated above. A total of 800 ug of protein (in 200 uL of buffer) was applied to a 5-30% sucrose gradient. The linear sucrose gradient was mixed using a Biocomp Gradient IP station (Biocomp, New Brunswick, Canada). After addition of the supernatant, the sucrose gradient was subjected to ultracentrifugation at 35,000 x g, for 14 hrs, at 4 °C (Beckman Coulter, Brea, CA). After centrifugation, fourteen 1 mL fractions were collected, and 12 µL of each fraction was resolved by SDS-PAGE using 4-20% gradient gels (Invitrogen, Carlsbad, CA). Following SDS-PAGE, proteins were transferred to nitrocellulose membranes for subsequent immunoblotting.

After resection of left ventricular free wall from 3- and 12-month-old mice hearts, tissues were further ground to powder in liquid nitrogen with SDS sample buffer (3.7 M Urea, 134.6 mM Tris, 5.4% SDS, 2.3% NP-40, 4.45% b-mercaptoethanol, 4% glycerol, 6mg/100ml bromophenol blue, PH6.8). The lysate was passed through a 26-gauge needle 10 times and then boiled for 3 min.

Standard procedures were used for SDS-PAGE and transferring to PVDF membrane. ENH antibody was purchased from Novus Biologicals (Littleton, CO) or was generously provided as gifts from Drs. Pascal Pomies (University of Montpellier, Montpellier, France) or Daniel Pak (Georgetown University, Washington, D.C.). Filamin C antibody was a gift from Dr. Louis M. Kunkel (Harvard Medical School, Boston, Massachusetts). Myotilin antibody was a gift from Dr. Olli Carpen (University of Helsinki, Helsinki, Finland). Integrin beta1D antibody was gift from Dr. Robert S. Ross (UCSD, La Jolla, CA). Commercial antibodies for α -actinin (Sigma-Aldrich, St. Louis, MO), Calsarcin-1 (Alpha Diagnostic International, San Antonio, TX), Desmin (Abcam, Cambridge, MA), GAPDH (Santa Cruz Biotechnology, Santa Cruz, CA), α B-crystallin (Stressgen, Ann Arbor, MI), were used. MAPK and phospho-MAPK family antibody sampler kits were from Cell Signaling (Danvers, MA). PKC and PKD1 antibodies were from Santa Cruz Biotechnology (Santa Cruz, CA) or Cell Signaling (Danvers, MA). Dystrophin antibody was from Spring Biosciences (Pleasanton, CA), Syntrophin was from Abcam (Cambridge, MA), γ -Sarcoglycan was from Vector Laboratories (Burlingame, CA).

***In vitro* Protein Interactions**

Protein interactions were studied *in vitro* as described before.⁹ Briefly, to explore the interaction between ENH and Calsarcin-1 or Myotilin, flag-tagged full-length Calsarcin-1 or Myotilin was cotransfected with HA-tagged ENH1/1a or ENH3/3b. For transfection experiments, HEK-293 cells were treated with lipofectamine 2000 (Invitrogen, Carlsbad, CA) according to the manufacturer's protocol. Transfected cells were harvested 24-30 hrs after transfection. Cells were suspended in RIPA buffer (Santa Cruz Biotechnology, Santa Cruz, CA), briefly sonicated, and clarified by centrifugation. The resultant supernatant was used for affinity gel purification. Expression of transient proteins were confirmed by western blot using anti-flag M2 (Sigma-Aldrich, St. Louis, MO) and anti-HA (Roche, Basel, Switzerland) antibodies. Anti-Flag M2 affinity gel (Sigma-Aldrich, St. Louis, MO) was used to pull down Flag-tagged proteins, and interacting proteins were visualized by western blot analysis using the anti-HA antibody.

Statistical analysis

All data are expressed as means \pm standard deviation (SD). We performed statistical analysis using Student's unpaired *t*-test. $P < 0.05$ was considered to be statistically significant.

Supplement Results

Generation of ENH-null Mice

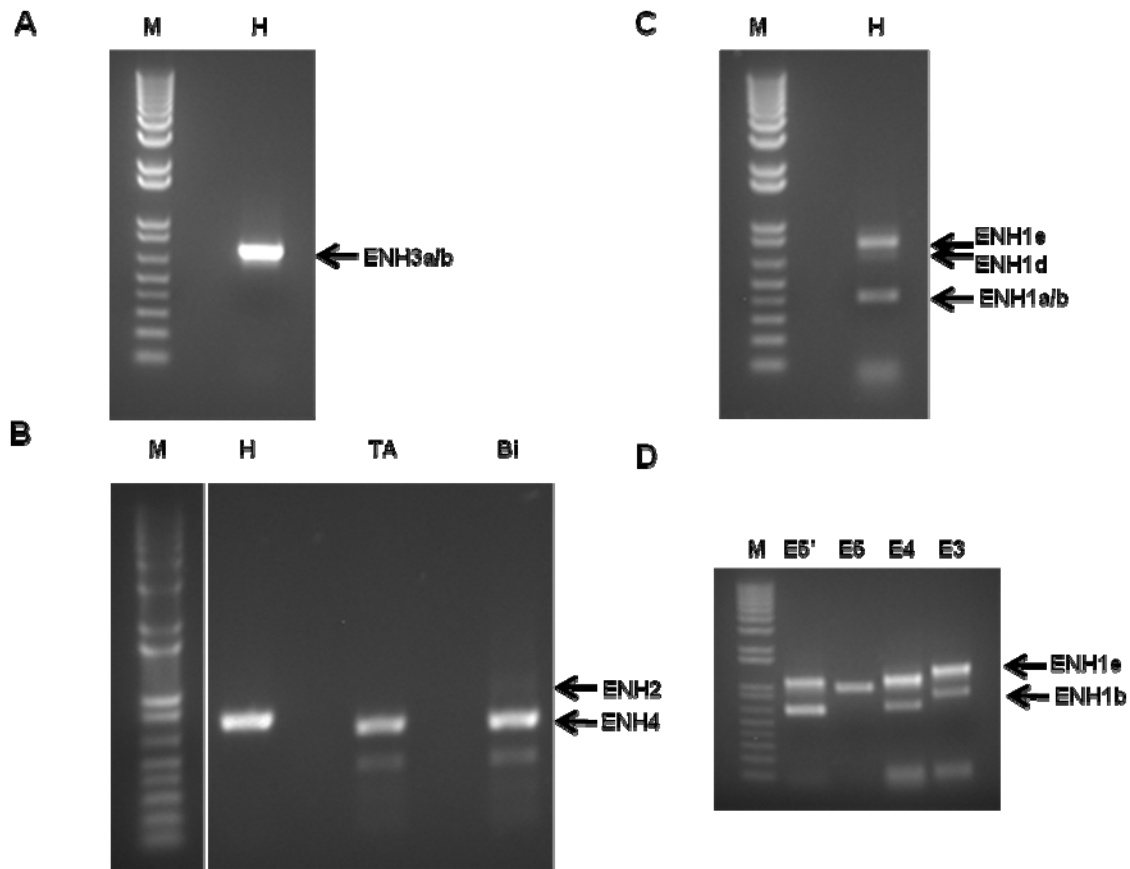
To investigate the *in vivo* biological role of ENH, we generated conditional ENH-null mice by targeting the third exon of the murine ENH gene (Online Figure II A). The third exon encodes part of the N-terminal PDZ domain present in all ENH splice isoforms. The targeting construct was linearized with restriction enzyme *Not I* and electroporated into R1 ES cells. Neomycin-resistant ES cells were analyzed by Southern blot analysis utilizing the 3'-probe as indicated in Online Figure II A. Successful homologous recombination was identified by the presence of bands at both 25 kb and 15 kb representing the WT and the targeted alleles, respectively (Online Figure II B). Chimera mice were produced by microinjection of 2 distinct positive ES clones into blastocysts from CL57BL/6J mice. Male chimera mice were bred with female Black Swiss mice. Germline transmission was confirmed by PCR and subsequent sequencing (see details in Supplement Methods). Homozygous Exon3-floxed mice (ENH^{fl/fl}) were crossed with protamine-Cre mice to generate *Cre* carrier mice (ENH^{fl/+, cre}). Male ENH^{fl/+, cre} mice were further bred with WT Black Swiss mice to get ENH heterozygous mice (ENH^{+/-}). Global ablation of all ENH isoforms (ENH^{-/-}) was achieved by intercrossing heterozygous mice. ENH protein expression in the heart was ablated in ENH-null (ENH^{-/-}) mice as shown by western blot analysis (Online Figure II C-E). We found that the ENH antibody from Abnova (PDLIM5 polyclonal antibody A02, H00010611-A02)¹¹ recognized Cypher and ENH isoforms, and all ENH isoforms were deleted in ENH^{-/-} hearts as indicated in Online Figure II C. The bands recognized by the Abnova antibody which correspond to the long and short Cypher isoforms were confirmed by using heart samples from global Cypher-null¹² and WT control mice (data not shown). As an additional confirmation, we confirmed the absence of the ENH short isoform by utilizing the ENH antibody from Dr. Pascal Pomies' lab¹³ (Online Figure II D). The ENH antibody from Dr. Daniel Pak's lab¹⁴ did not recognize Cypher and also showed complete deletion of ENH in ENH^{-/-} hearts (Online Figure II E). Thus, we have successfully generated ENH knockout mice.

References for Supplemental Methods

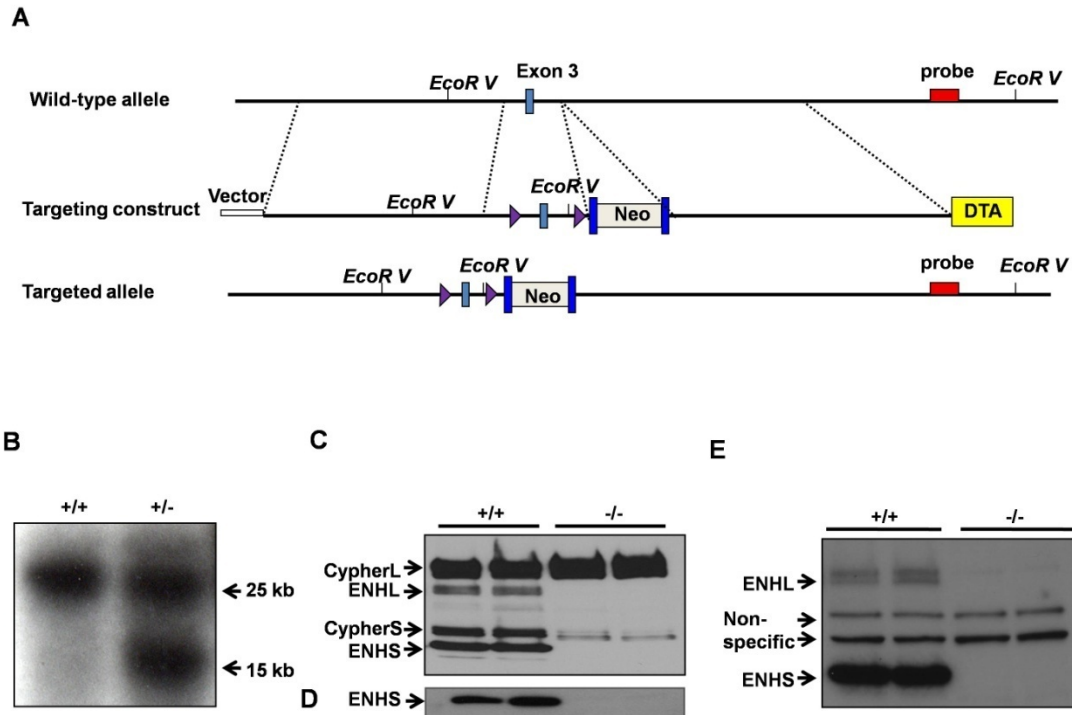
1. Liang X, Zhou Q, Li X, Sun Y, Lu M, Dalton N, Ross J, Jr., Chen J. PINCH1 plays an essential role in early murine embryonic development but is dispensable in ventricular cardiomyocytes. *Mol Cell Biol.* 2005;25:3056-3062.
2. O'Gorman S, Dagenais NA, Qian M, Marchuk Y. Protamine-Cre recombinase transgenes efficiently recombine target sequences in the male germ line of mice, but not in embryonic stem cells. *Proc Natl Acad Sci U S A.* 1997;94:14602-14607.
3. Jiao K, Kulesa H, Tompkins K, Zhou Y, Batts L, Baldwin HS, Hogan BL. An essential role of Bmp4 in the atrioventricular septation of the mouse heart. *Genes Dev.* 2003;17:2362-2367.
4. Tanaka N, Dalton N, Mao L, Rockman HA, Peterson KL, Gottshall KR, Hunter JJ, Chien KR, Ross J, Jr. Transthoracic echocardiography in models of cardiac disease in the mouse. *Circulation.* 1996;94:1109-1117.
5. Bale TL, Hoshijima M, Gu Y, Dalton N, Anderson KR, Lee KF, Rivier J, Chien KR, Vale WW, Peterson KL. The cardiovascular physiologic actions of urocortin II: acute effects in murine heart failure. *Proc Natl Acad Sci U S A.* 2004;101:3697-3702.
6. Rockman HA, Ross RS, Harris AN, Knowlton KU, Steinhilper ME, Field LJ, Ross J, Jr., Chien KR. Segregation of atrial-specific and inducible expression of an atrial natriuretic factor transgene in an in vivo murine model of cardiac hypertrophy. *Proc Natl Acad Sci U S A.* 1991;88:8277-8281.
7. Jones WK, Grupp IL, Doetschman T, Grupp G, Osinska H, Hewett TE, Boivin G, Gulick J, Ng WA, Robbins J. Ablation of the murine alpha myosin heavy chain gene leads to dosage effects and functional deficits in the heart. *J Clin Invest.* 1996;98:1906-1917.
8. Zhang J, Bang ML, Gokhin DS, Lu Y, Cui L, Li X, Gu Y, Dalton ND, Scimia MC, Peterson KL, Lieber RL, Chen J. Syncoilin is required for generating maximum isometric stress in skeletal muscle but dispensable for muscle cytoarchitecture. *Am J Physiol Cell Physiol.* 2008;294:C1175-1182.
9. Zheng M, Cheng H, Li X, Zhang J, Cui L, Ouyang K, Han L, Zhao T, Gu Y, Dalton ND, Bang ML, Peterson KL, Chen J. Cardiac-specific ablation of Cypher leads to a severe form of dilated cardiomyopathy with premature death. *Hum Mol Genet.* 2009;18:701-713.
10. Solaro RJ, Pang DC, Briggs FN. The purification of cardiac myofibrils with Triton X-100. *Biochim Biophys Acta.* 1971;245:259-262.
11. Gardezi SR, Weber AM, Li Q, Wong FK, Stanley EF. PDLIM5 is not a neuronal CaV2.2 adaptor protein. *Nat Neurosci.* 2009;12:957-958; author reply 958.
12. Zhou Q, Chu PH, Huang C, Cheng CF, Martone ME, Knoll G, Shelton GD, Evans S, Chen J. Ablation of Cypher, a PDZ-LIM domain Z-line protein, causes a severe form of congenital myopathy. *J Cell Biol.* 2001;155:605-612.
13. Niederlander N, Fayein NA, Auffray C, Pomies P. Characterization of a new human isoform of the enigma homolog family specifically expressed in skeletal muscle. *Biochem Biophys Res Commun.* 2004;325:1304-1311.
14. Herrick S, Evers DM, Lee JY, Udagawa N, Pak DT. Postsynaptic PDLIM5/Enigma Homolog binds SPAR and causes dendritic spine shrinkage. *Mol Cell Neurosci.* 2010;43:188-200.

Online Table I: The three new identified exons for mouse ENH gene. The exon sequences are in red and the flanked 20-bp intron sequences are in black. The splice donor and acceptor sites are underlined.

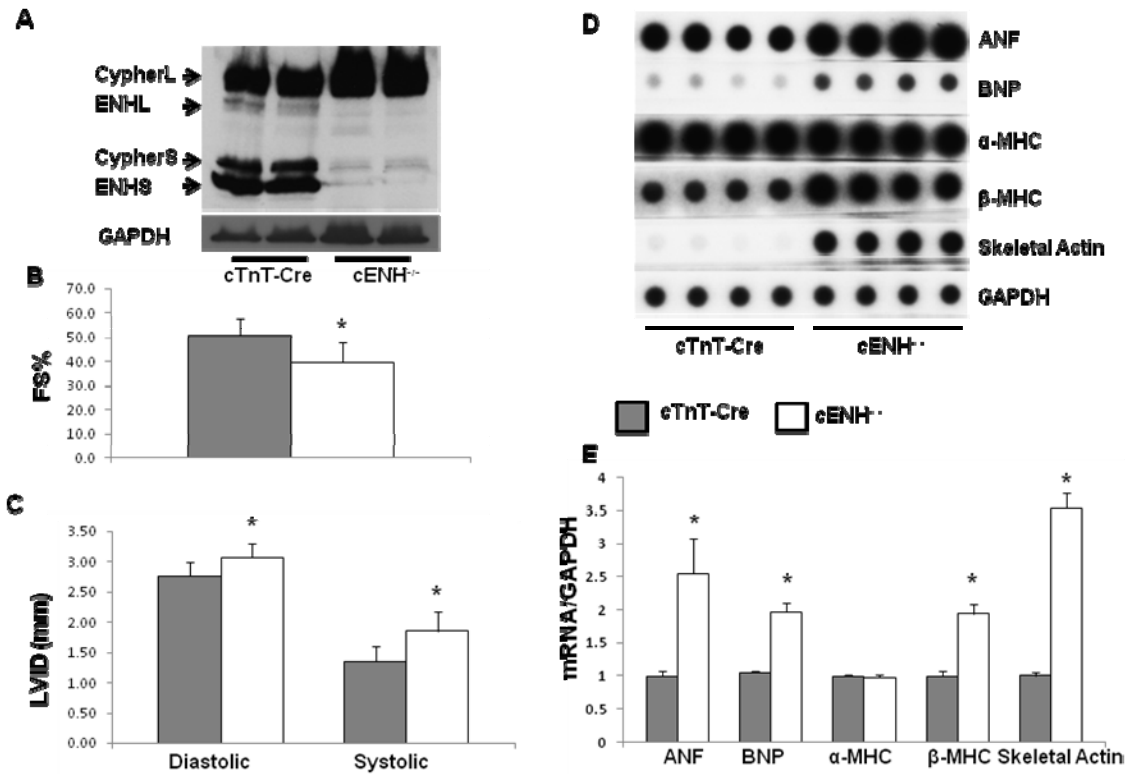
Exon 12 (120 bp)	TTTTACTTCTGAAA <u>CTTAG</u> GTTTTACAGTTCTCTGGAAGACCCCCTTAAGA ACGGACCACACCCACCTGCAGCTCCCAGCTGTTAAAAGTTCATAGTCAAGT AGCCATAGTTTCTAAGGAAGCAGCCACTTACTCTAG <u>GT</u> AGAGTTCTTTTTCC ATTT
Exon 13 (144 bp)	GTCTTTTTTCCCTGTCA <u>AGT</u> GTAAGCAGGTCTACAAGAACTGTAGAAGGTG CTTTGGAAGGCTTTGGAAACTTTCCTGCCTTCTCCCCTCCTACTAGATACAGT GCTGTAGTCGTCAGTGATGCGGCTGCCACTGTGTCTGCTGCTCTCGCTGCGA AAACCAG <u>G</u> TAGAATTATGTGTGCAGTA
Exon 14 (132 bp)	CCTCTCTGAATGCTTGCCAG <u>G</u> CTCTTCGGCCCTGAAAACCTCCAGTCTCTTCT GGATGCACTGTGCATCAGCACTGTCCCAAGCCTCTAGCTCTTTCCTGTCTTC AGTCCTCTGAGGAGTCGAGTGGCTCTGTCCACGTTAAGAAGAGCAG <u>G</u> TACT ATGGAGGGACCATGG



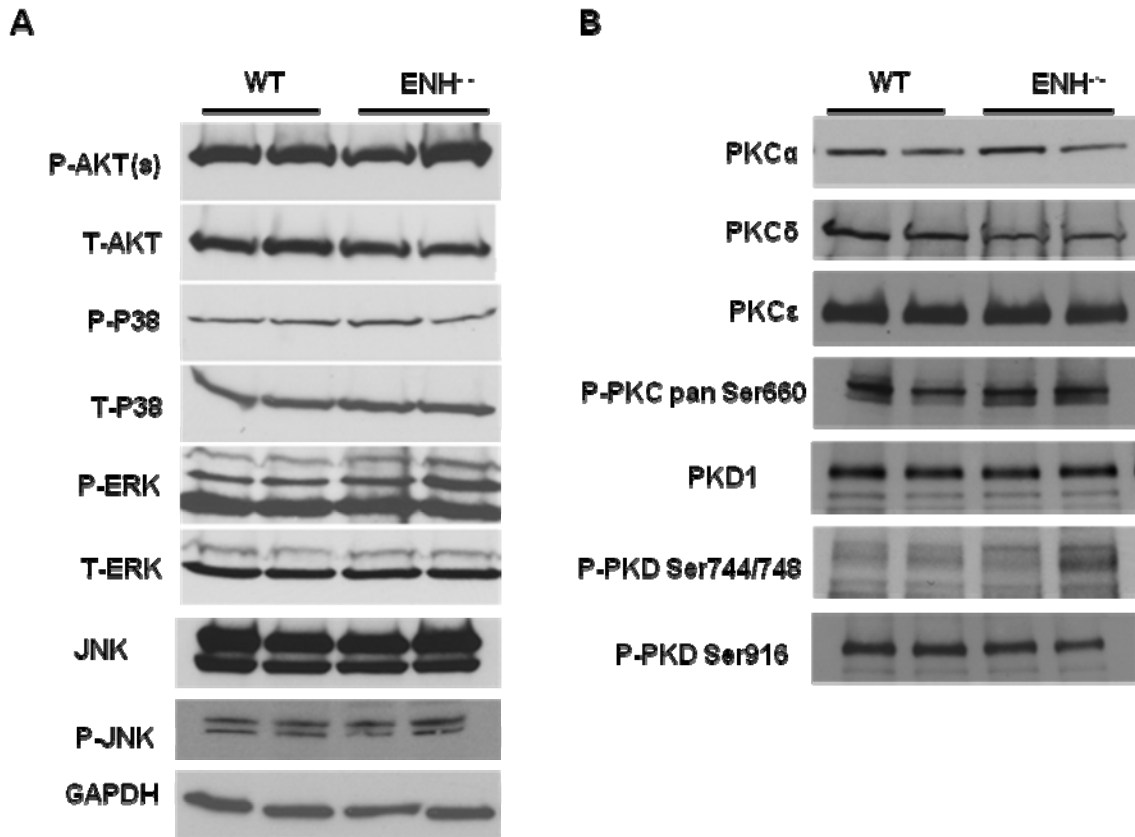
Online Figure I: ENH splice isoforms. A, ENH short isoforms (ENH3) in mouse heart (H) was amplified using primers of ENH-SF and ENH-SR (see Materials and Methods). 1 kb plus DNA ladder was used as DNA marker (M). DNA sequencing results showed that 4 for ENH3a (702 bp) and 7 for ENH3b (717 bp) in total 11 different sequences. B: ENH short isoforms in mouse heart (H) and skeletal muscle were amplified as in A. ENH4 (642 bp) is the main ENH isoform in tibialis anterior muscle (TA) and biceps muscle (Bi). ENH2 (1011 bp) is detectable in biceps (Bi) muscle. C: PCR products amplified from mouse heart using ENHE9 and ENHE16 as primers. ENH1a/b (404 bp) and ENH1e (800 bp) are the major long isoforms in the mouse heart. ENH1d (676 bp) is also detectable. D: New exons (exon 12-14) were together with exon 5' not exon 5 in ENH long splice isoforms. Primers designed in exon3 (1227 bp for ENH1e and 831 bp for ENH1b), 4 (1078 bp for ENH1e and 682 bp for ENH1b), 5 (only 960 bp for ENH1a) and 5' (1035 bp for ENH1e and 639 bp for ENH1b) with primer in exon 16 (ENHE16) were used.



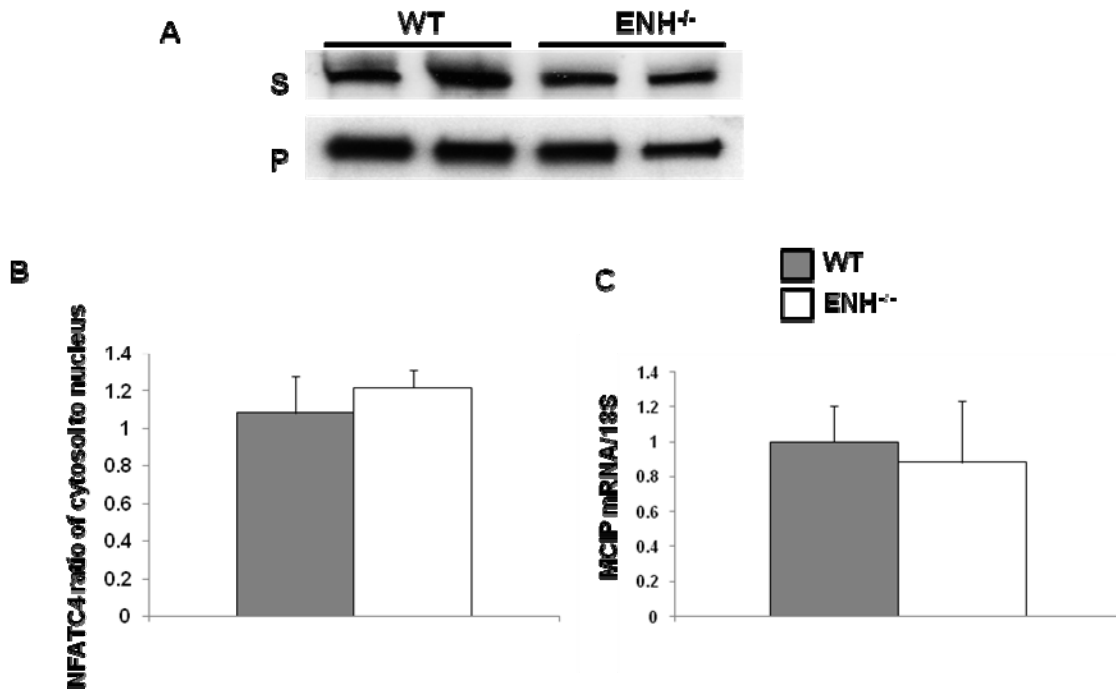
Online Figure II: Generation of $ENH^{-/-}$ mice. A, The third exon of the mouse ENH gene was floxed by two *loxP* sites (triangle) in Pflox-FRT-neo vector. The neomycin cassette (Neo) flanked by two FRT sites (blue rectangle) was inserted into the third intron of the mouse ENH gene. Restriction enzyme *EcoRV* was used to digest genomic DNA isolated from mouse ES cells for Southern blot analysis. Probe sequence was designed downstream of the 3' recombinant arm as shown (red rectangle). DTA (diphtheria toxin, yellow rectangle) cassette was fused to the terminal of 3' arm to assist in homologous recombination. B, Representative Southern blot shows band at 25 kb for WT allele and 15 kb for targeted allele. C-E, western blot analysis shows complete deletion of ENH protein in $ENH^{-/-}$ hearts using various ENH antibodies from Abnova (C) and Drs. Pascal Pomies (D) and Daniel T.S. Pak (E).



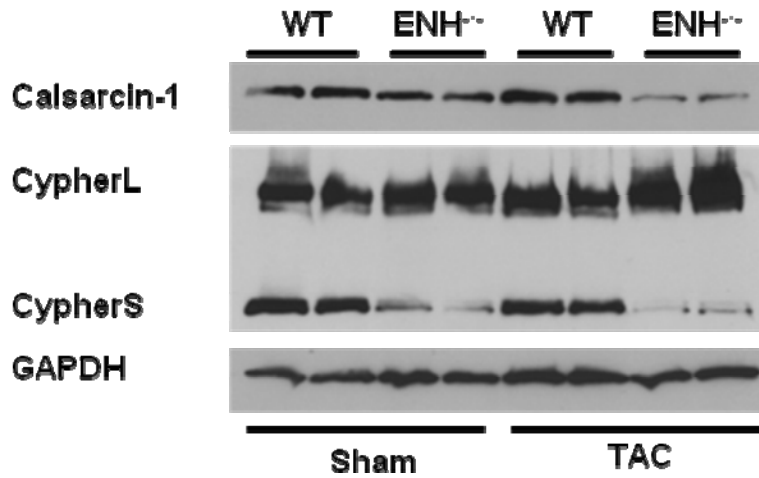
Online Figure III: Dilated cardiomyopathy in ENH cardiac-specific knockout (cENH^{-/-}) mice. A, The ENH protein, detected by ENH antibody from Abnova, is dramatically deleted in the ENH cardiac specific knockout hearts at 5-months. B and C, Enlargement of the left ventricle as measured by LVID (* P < 0.05) at end of diastole and systole and reduced heart contractility represented as %FS (* P < 0.05) were assessed by echocardiography for the cENH^{-/-} mice (n=8, blank) and Troponin T-Cre carrier mice (TnT-Cre) (n=8, grey) at 3-months. D, The levels of cardiac fetal genes (ANF, BNP, β-MHC and skeletal Actin) were upregulated in cENH^{-/-} mice at 5-months as shown by dot-blot analysis. GAPDH was used as a RNA loading control. E, Quantitative data from D standardized to GAPDH are shown (* P < 0.05).



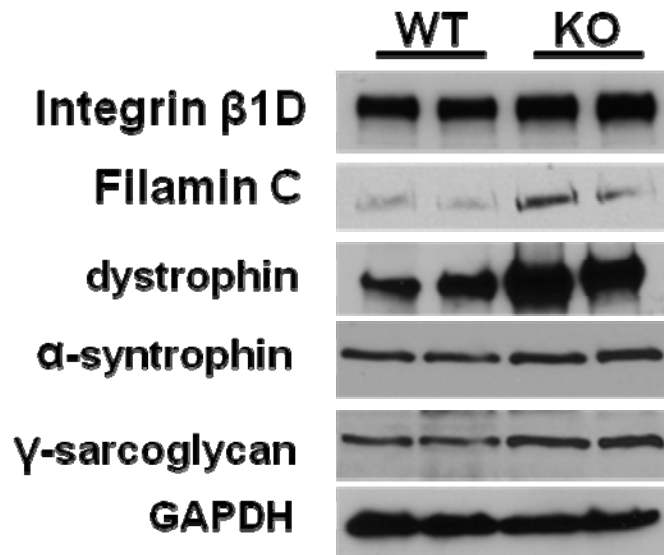
Online Figure IV: Cell signaling pathways in ENH null hearts. A: The AKT and MAP kinase pathway (p38, ERK and Jnk) were not differentially activated in ENH^{-/-} mice compared with WT at 3-months. B: Both total proteins and active forms of PKC α , δ , ϵ and PKD1 did not alter in 3-month-old ENH^{-/-} hearts. GAPDH was used as loading control.



Online Figure V: Calcineurin-NFAT pathway was not activated in ENH null hearts. A: Representative western blot show the NFATC4 protein in cytosolic and nuclear fractions in wild-type and ENH null hearts. B: The nucleus to cytosol ratios of NFATC4 was calculated after reading the grey densities using ImageJ software. C: Real time PCR result showed same MCIP mRNA level between WT and ENH null hearts.



Online Figure VI: Extra downregulation of Calsarcin and CypherS in ENH null hearts following biomechanical stress. WT or ENH null mice were under either sham operation or TAC surgery for 4 weeks. GAPDH was used as protein loading control.



Online Figure VII: Integrin, Filamin C and Dystrophin glycoprotein complex were upregulated in $ENH^{-/-}$ hearts. Integrin β 1D, Dystrophin, Syntrophin and Sarcoglycan antibodies were used to blot both WT and $ENH^{-/-}$ heart tissues. GAPDH was used as protein loading control.